nature biomedical engineering

SUPPLEMENTARY INFORMATION

https://doi.org/10.1038/s41551-019-0378-3

In the format provided by the authors and unedited.

Visualization of early events in mRNA vaccine delivery in non-human primates via PET–CT and near-infrared imaging

Kevin E. Lindsay[1,5], Sushma M. Bhosle[1,5], Chiara Zurla[1,5], Jared Beyersdorf[1], Kenneth A. Rogers[2], Daryll Vanover[1], Peng Xiao[2], Mariluz Araínga[2], Lisa M. Shirreff[2], Bruno Pitard[3], Patrick Baumhof[4], Francois Villinger[2] and Philip J. Santangelo[1]*

[1]Wallace H. Coulter Department of Biomedical Engineering, Georgia Tech and Emory University, Atlanta, GA, USA. [2]New Iberia Research Center, University of Louisiana at Lafayette, Lafayette, LA, USA. [3]CRCINA, INSERM, University of Nantes, University of Angers, Nantes, France. [4]CureVac AG, Tübingen, Germany. [5]These authors contributed equally: Kevin E. Lindsay, Sushma M. Bhosle, Chiara Zurla. *e-mail: philip.santangelo@bme.gatech.edu

Table of contents

Suppl. Fig 1: Excised inguinal lymph node from animal AFO32. Analysis of the isolated organ using the portable near IR camera showed that only a well demarcated portion of its volume was positive for mRNA signal

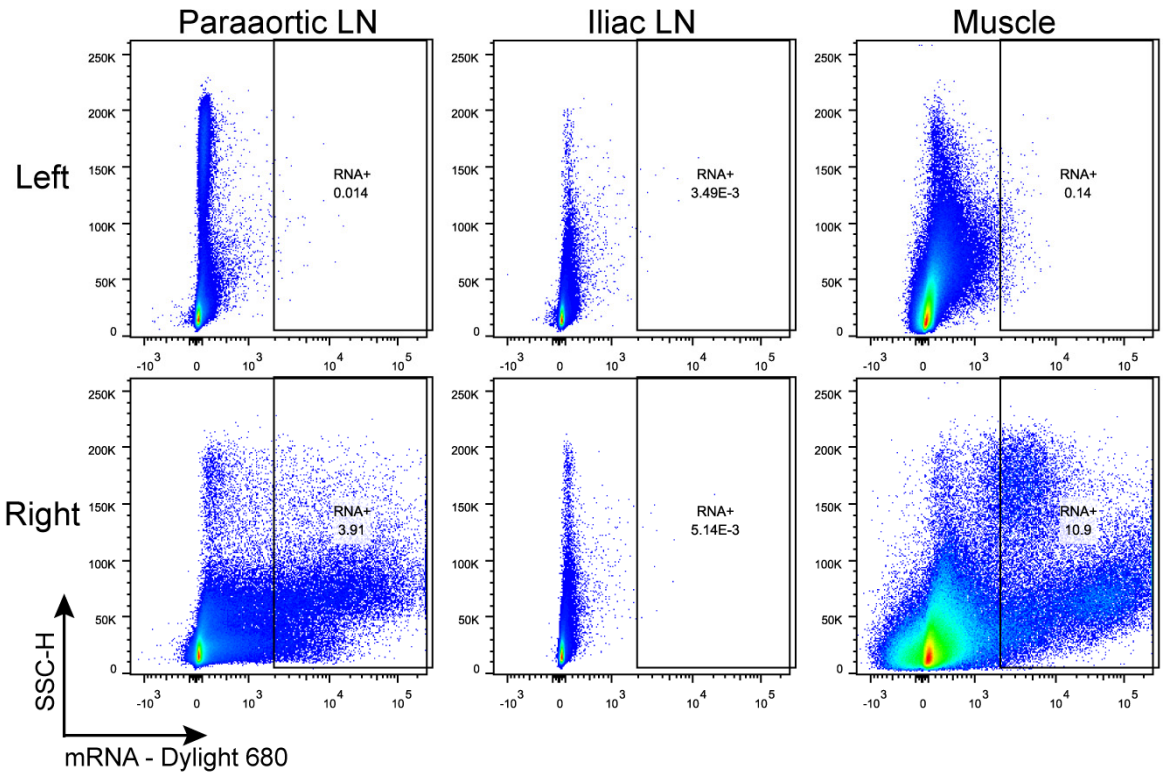

Suppl. Fig.2: Total mRNA+ Cells in the muscles and draining LNs of CM-653. After gating for cells and removing doublets, the plots show the total number of mRNA+ cells identified in each tissue by flow cytometry. Right: ipsilateral, left:contralateral. n=1

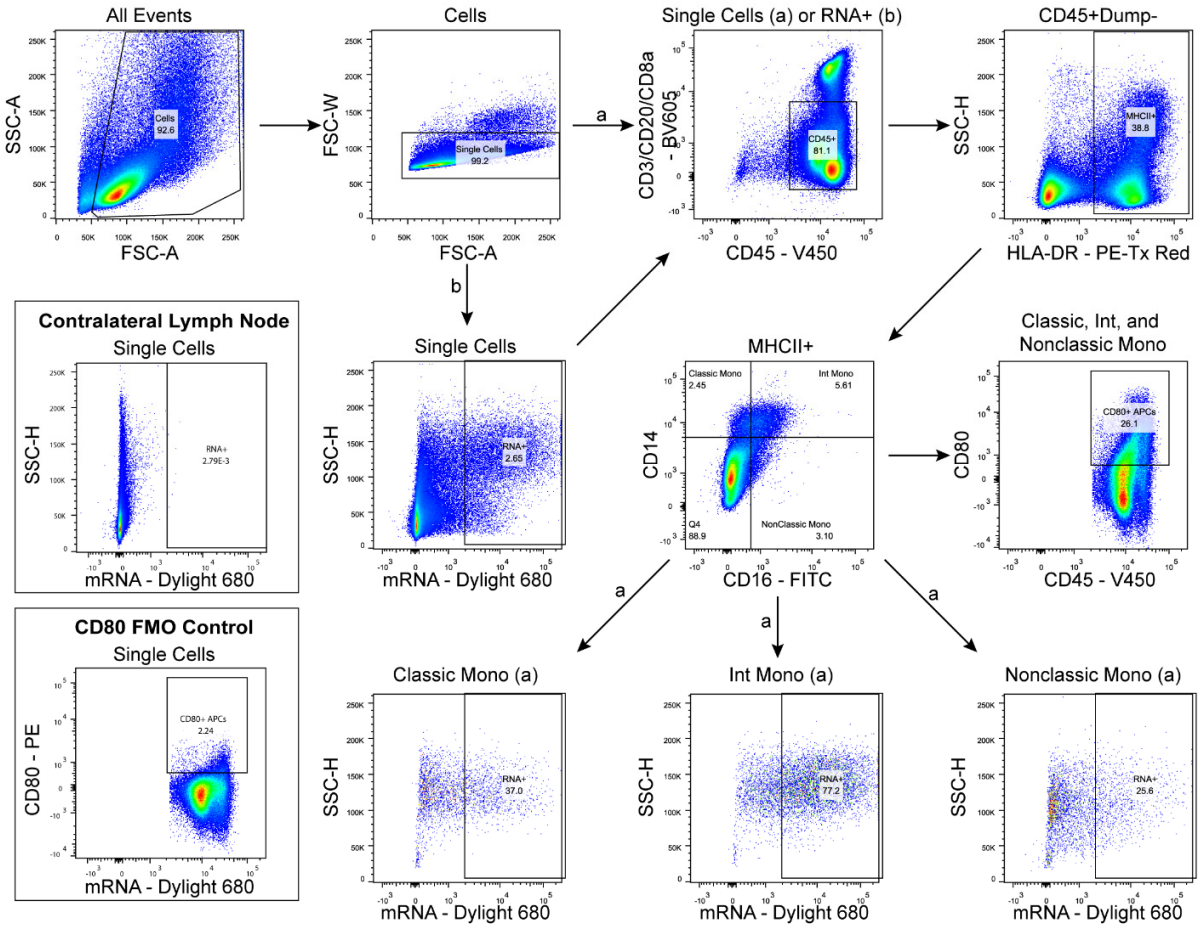

Suppl Fig. 3 Gating Strategy for Monocyte Subtypes. Cell suspensions obtained from processed muscle or lymph nodes were stained with indicated antibodies (Suppl.Tables 2-3). The data from each tissue were analyzed using two gating paths: cell type followed by mRNA uptake (path a) or mRNA uptake followed by cell type (path b). Arrows used in paths a or b are labeled. Unlabeled arrows are used in both gating paths. The gating scheme was adapted from Kasturi et al.[1] Classical monocytes, intermediate monocytes, and nonclassical monocytes were identified as CD14+CD16-, CD14+CD16+, and CD14-CD16+, respectively. Data shown are from analysis of the ipsilateral (right) paraaortic lymph node. Boxed plots depict data from contralateral paraaortic lymph node to show gating limits for RNA+ cells and a CD80 FMO control sample to show gating limits for CD80+ cells.

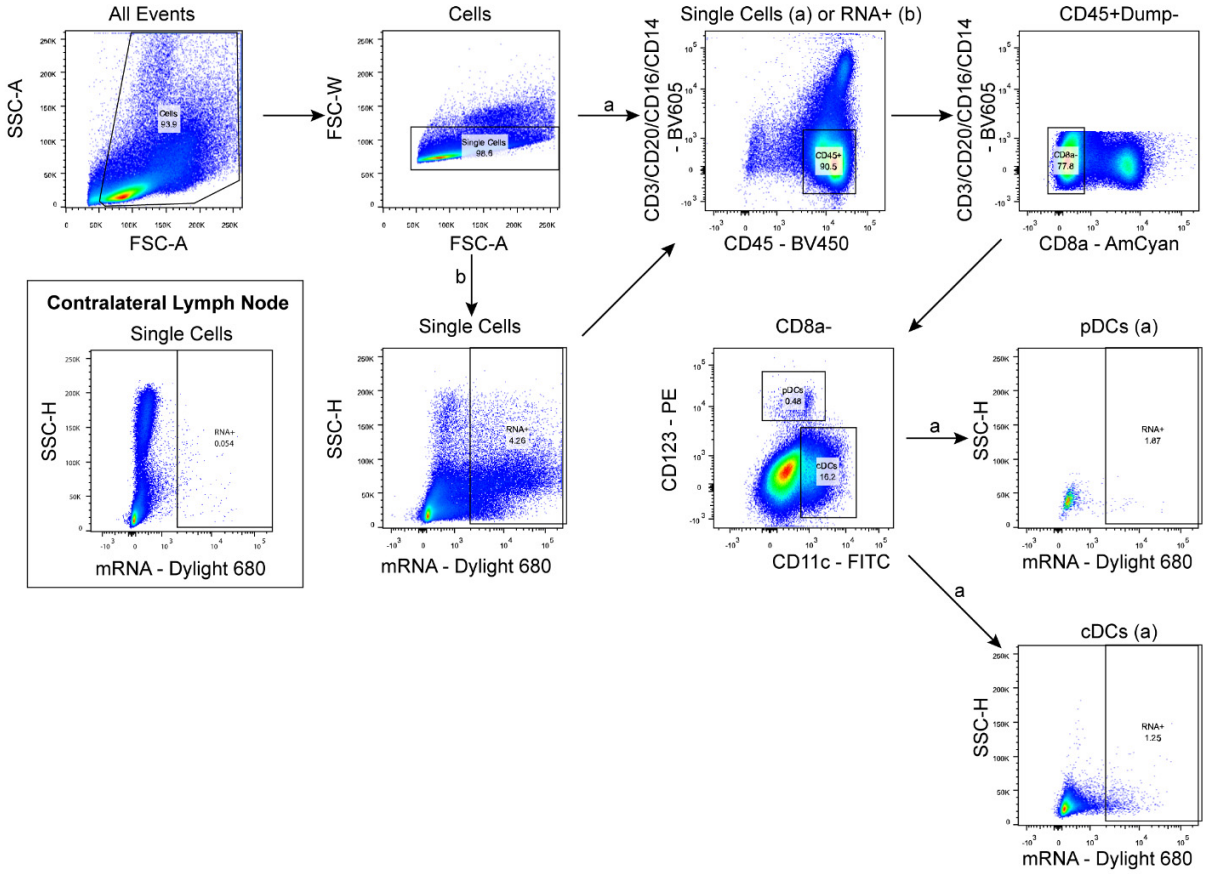

Suppl. Fig. 4 Gating Strategy for Conventional and Plasmacytoid Dendritic Cells. Cell suspensions obtained from processed muscle or lymph nodes were stained with antibodies indicated in Suppl. Tables 2-3. The data from each tissue were analyzed by two gating paths: cell type followed by mRNA uptake (path a) or mRNA uptake followed by cell type (path b). Arrows used in path a or b are labeled. Unlabeled arrows are used in both gating paths. Gating scheme was adapted from Kasturi et al [1] Data shown are from analysis of the ipsilateral (right) paraaortic lymph node. Boxed plot depicts data from contralateral paraaortic lymph node to show gating limits for RNA+ cells.

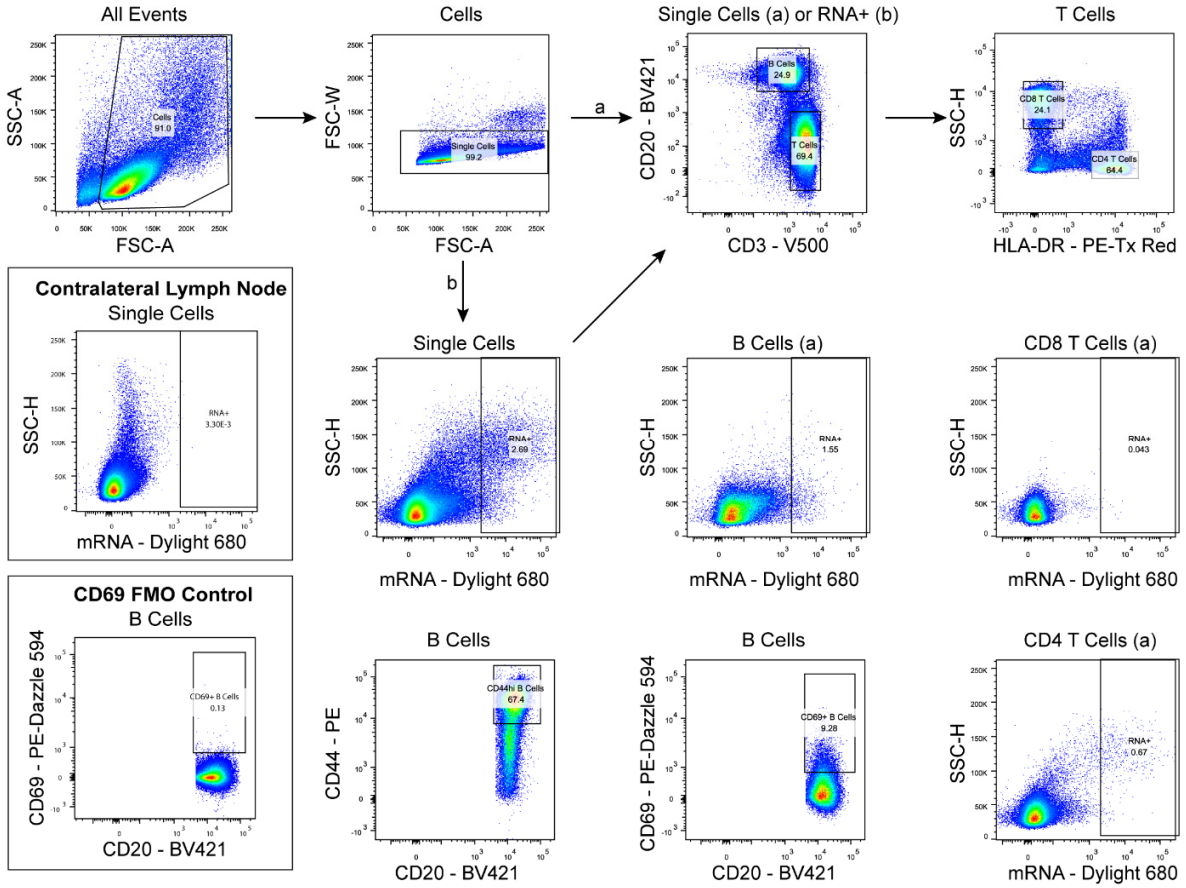

Suppl. Fig. 5 Gating Strategy for T and B Cells. Cell suspensions obtained from processed muscle or lymph nodes were stained with antibodies indicated in Suppl Tables 2-3. The data from each tissue were analyzed by two gating paths: cell type followed by mRNA uptake (path a) or mRNA uptake followed by cell type (path b). Arrows used in path a or b are labeled. Unlabeled arrows are used in both gating paths. Gating for CD44hi and CD69+ cells was performed for B cells, CD4 T Cells, and CD8 T Cells. Data shown are from analysis of the ipsilateral (right) paraaortic lymph node. Boxed plots depict data from contralateral paraaortic lymph node to show gating limits for RNA+ cells and a CD69 FMO control sample to show gating limits for CD69+ cells.

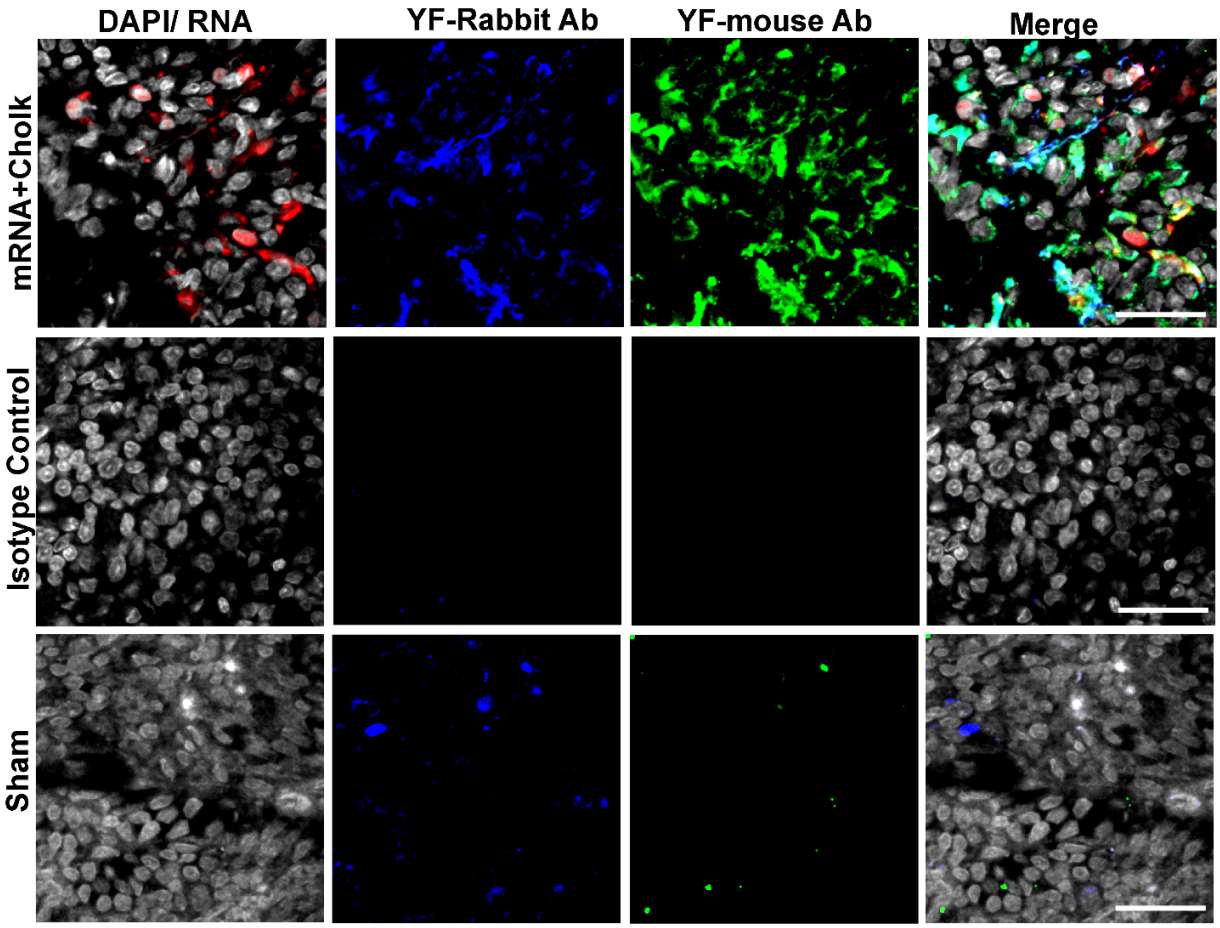

Suppl. Fig 6 Detection of Yellow fever prME protein expression with two different antibodies in a macaque iliac lymph node: Lymph node tissue sections were stained with a YF antibody raised in mouse (blue) and rabbit (green). mRNA is shown in red and DAPI in white. Images were aquired on a Zeiss 780 confocal microscope with a 40X objective. Scale bars are 30 µm. Representative images are shown (n=3).

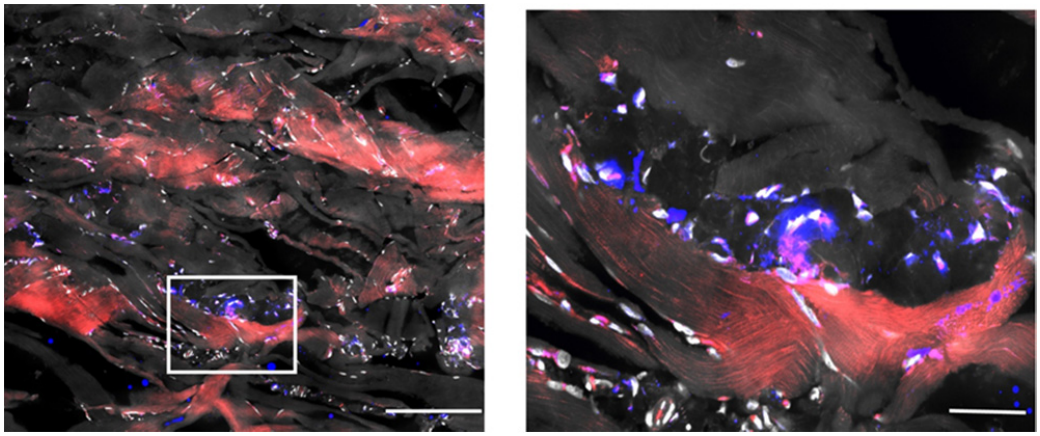

Suppl. Fig 7: Yellow fever prME mRNA and protein expression in muscle. Ipsilateral muscle stitched image was aquired on a Zeiss 780 confocal microscope with a 40X objective demonstrating mRNA and protein distribution in blue and red, respectively; the DAPI signal was purposely contrast enhanced to visualize muscle fibers. Scale bar is 200 µm. Magnification of boxed area. Scale bar is 50 µm. Representative images are shown (n=3).

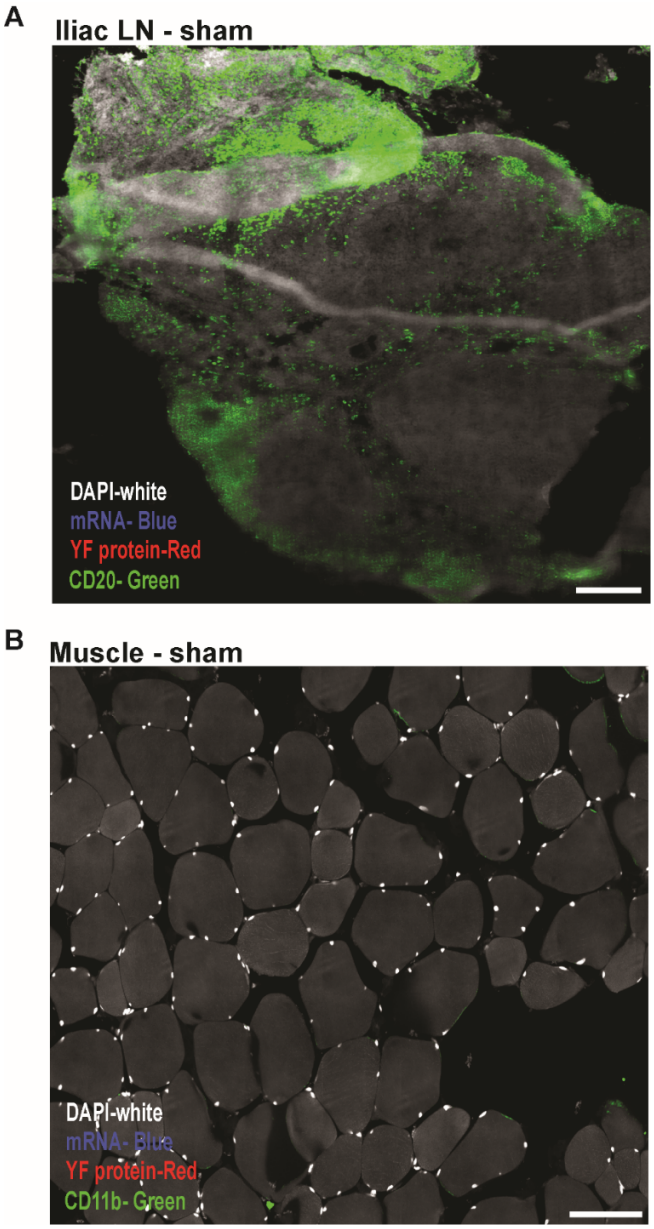

Suppl. Fig 8: Stitched images for iliac LN and muscle from uninjected controls. (A) Stitched image of sham Iliac LN stained for the YF protein (red) and the cell type marker CD20 (green). Images were aquired on a Zeiss 780 confocal microscope with a 20X objective. Scale bar is 200 µm. (B) Stitched image of sham muscle stained for YF protein (red) and the cell type marker CD11b (green). Images were aquired on an Elyra confocal microscope with a 40X objective. Scale bar is 100 µm. mRNA is shown in blue and DAPI in white. Representative images are shown (n=3).

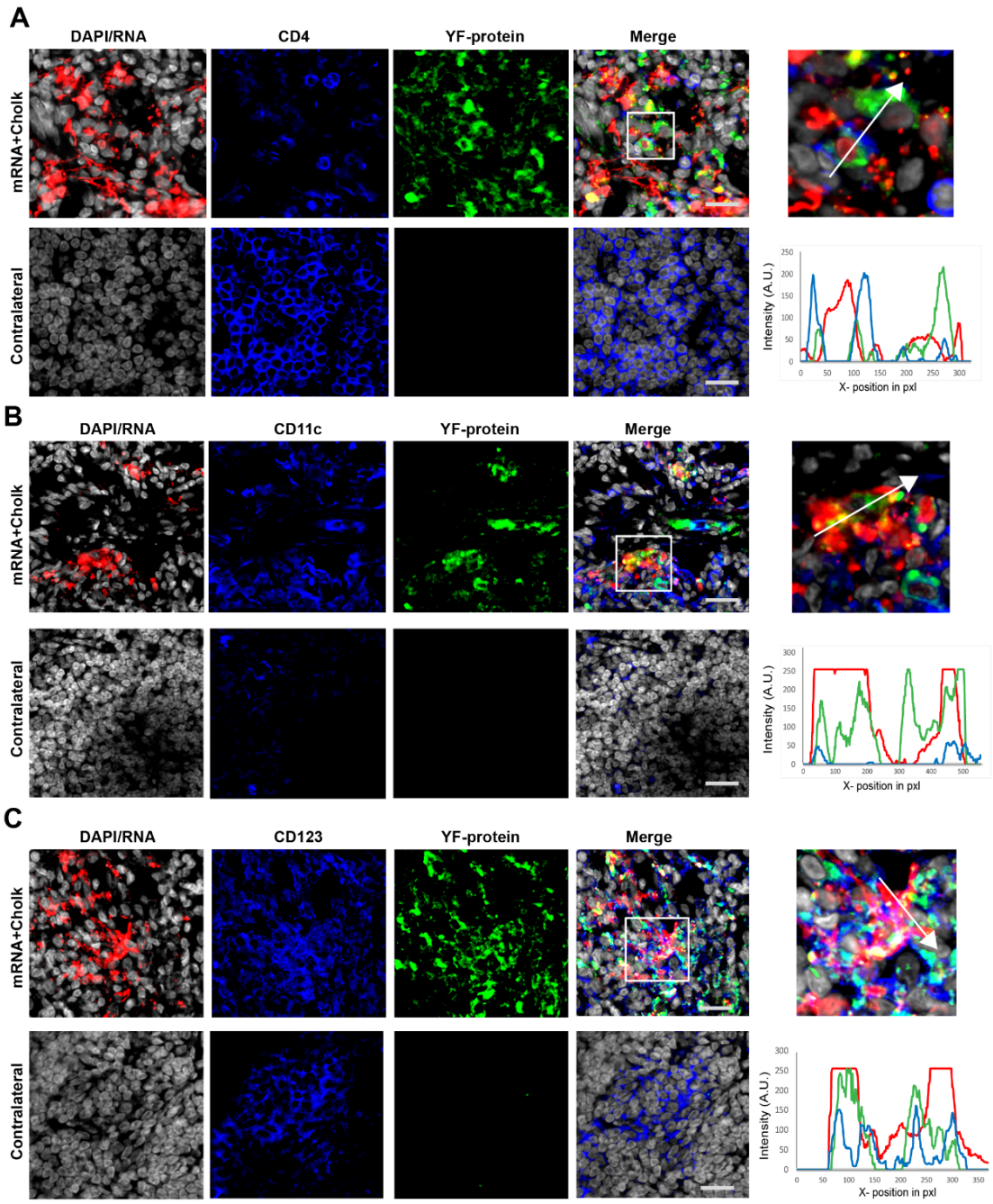

Suppl. Fig 9: Yellow fever prME mRNA and protein expression in lymph node immune cells. Lymph node tissue sections were stained with the immune cell markers (blue) CD4 (A), CD11c (B) and CD123 (C), YF prME protein (green) and counterstained for DAPI (white). Controls from uninjected monkeys are shown. Images were acquired on a Zeiss 780 confocal microscope with a 40X objective. Scale bars are 50 µm. Line

profiles for cropped images indicate mRNA in red, cell marker in blue and protein in green. Representative images are shown (n=3).

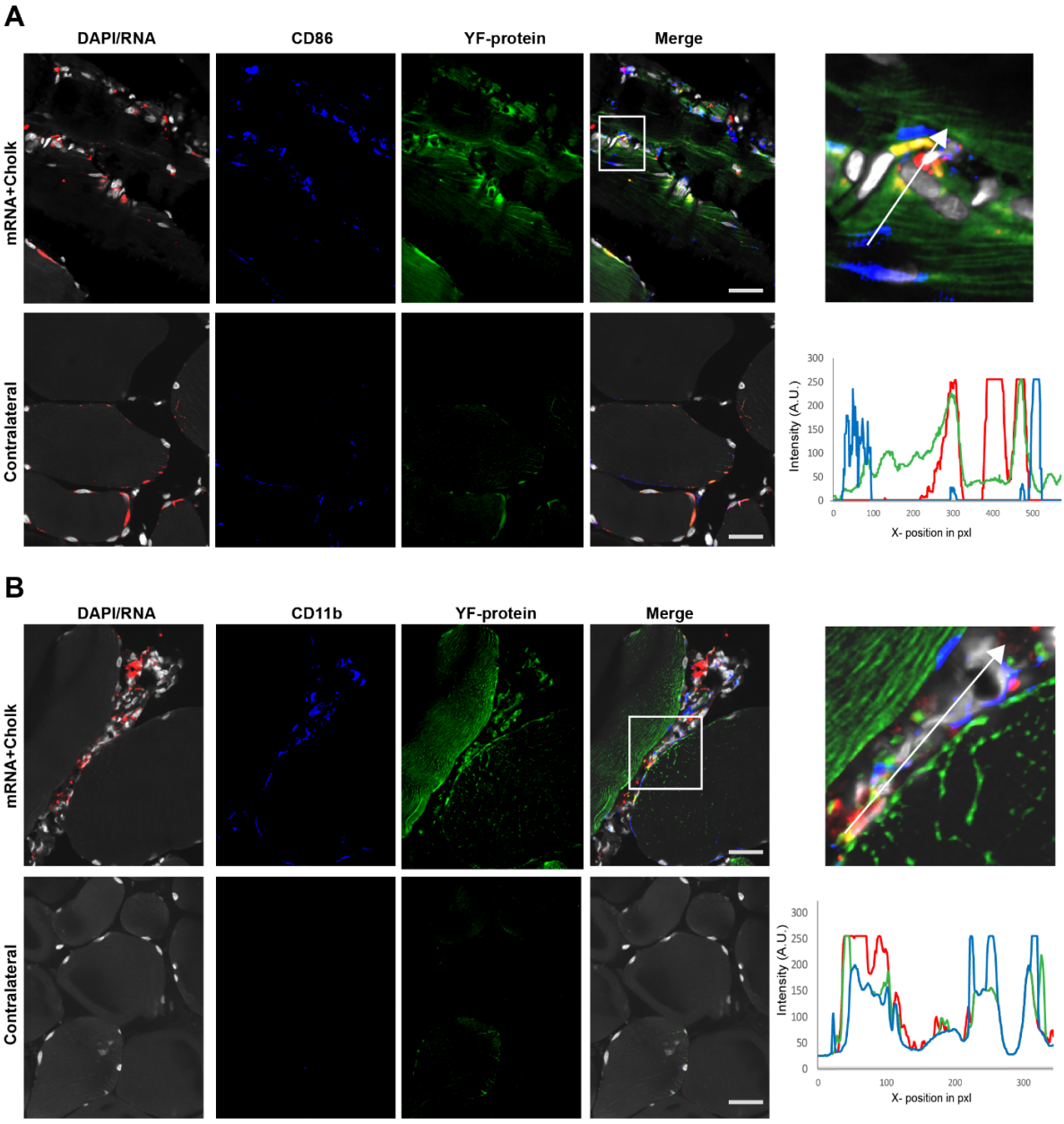

Suppl. Fig 10: Infiltrating immune cells (APCs, Macrophages) and YF prME protein at site of injection. Injected and contralateral muscles stained for YF protein in green, immune cell markers in blue [CD86 (A) and CD11b (B)]. mRNA is shown in red and DAPI in white. Images were acquired on a Zeiss 780 confocal microscope with 40X objective. Scale bars are 50 µm. Line profiles for cropped images indicate mRNA in red, cell marker in blue and protein in green. Representative images are shown (n=3).

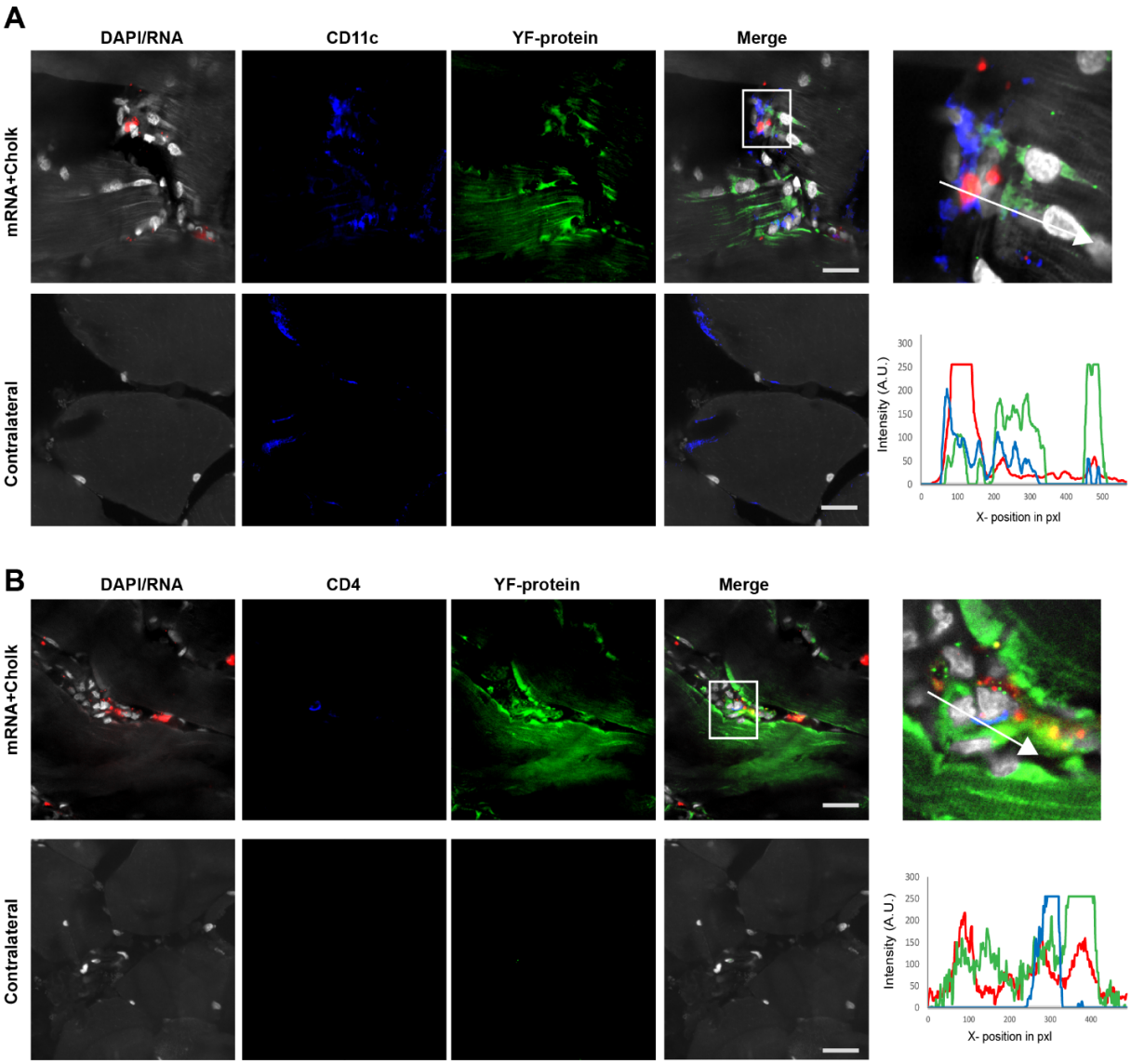

Suppl. Fig 11: Infiltrating immune cells (DCs, T cells) and YF prME protein in muscle tissue. Injected and contralateral muscle tissues stained for YF protein in green and immune cell markers in blue [CD11c (A) and CD4 (B)], mRNA is shown in red and DAPI in white. Images were acquired on an Zeiss 780 confocal microscope with 40X objective. Scale bars are 50 µm. Line profiles for cropped images indicate mRNA in red, cell marker in blue and protein in green. Representative images are shown (n=3).

Tables:

Table 1: Total SUV values, radioactivity, fluorescence, percentage of RNA positive cells and of activated intermediate monocytes in animal CM-653 24 hours post injection. The values in parenthesis refer to results obtained by the analysis of contralateral organs.

	Total SUV	Geiger counts (µCi)	Fluobeam (+/-)	% RNA+ cells	% activated monocytes
Muscle	9412	248 (0)	+	10.9 (0.14)	24.5 (21.7)
Inguinal LN	100	0 (0)	-	N/A	N/A
Iliac LN	12	0 (0)	-	0.01 (0.00)	45.7 (29.4)
Paraaortic LN	988	28 (0)	+	3.91 (0.01)	63 (59)

Table 2: Details of flow cytometry panels used to characterize RNA positive cell types in the muscle and draining LN of animal CM-653

Channel	T and B	DCs	Monocytes
1	CD4 BV605	CD3, CD20, CD16, CD14 BV605	CD3 CD20, and CD8a BV605
2	CD3 V500	CD8a Amcyan	CD14 V500
3	CD20 BV421	CD45 v450	CD45 V450
4	CD69 PE-Dazzle594	HLA-DR PE-Tx red	HLA-DR PE-Tx red
5	CD44PE	CD123 PE	CD80 PE
6	CD8 FITC	CD11c FITC	CD16FITC
7	mRNA Dylight 680	mRNA Dylight 680	mRNA Dylight 680

Table 3: List of antibodies used for flow cytometry

	List of antibodies	Clone	Maunfacture	Cat#
BV605	CD4	OKT4	BioLegend	317438
	CD3	SP34-2	BD	562994
	CD20	2H7	BD	563783
	CD16	3G8	BioLegend	302040
	CD14	M5E2	BioLegend	301834
	CD8a	SK1	BD	564116
V500	CD3	SP34-2	BD	560770
	CD14	M5E2	BD	561391
AmCyan	CD8a	SK1	BD	339188
BV421	CD20	2H7	BD	562873
V450	CD45	D058-1283	BD	561294
PE-Dazzle594	CD69	FN50	BioLegend	310942
PE-Tx-Red	HLA-DR	TU36	Life technologies	MHLDR17
PE	CD44	IM7	BioLegend	103024
	CD123	7G3	BD	554529
	CD80	L307.4	BD	557227
FITC	CD8a	RPA-T8	BD	555366
	CD11c	3.9	BioLegend	301604
	CD16	3G8	BioLegend	302006

Table 4: List of antibodies used for immunofluorescence.

Cell Marker	Primary antibody Host (source) / Dilution in blocking soln.	Secondary antibody (source) / Dil. In blocking soln.	Primary Antibody cat. No. / clone
CD86 – Antigen presenting cells	Rabbit (Abcam) / 1:50	Donkey anti rabbit-488 (Invitrogen) /1: 500	ab53004 / EP1158Y
CD20- B cells	Rabbit(Abcam) / 1:50	Donkey anti rabbit-488(Invitrogen) /1: 500	ab78234 / EP459Y
CD68-Macrophages	Rabbit (Santacruz)/ 1:25	Donkey anti rabbit-488(Invitrogen) /1: 500	sc-9139 / H-255
YF protein	Mouse (Sigma)/ 1:2000	Donkey anti mouse 555 (Invitrogen) /1:500	MAB984 / 2D12.A
CD123 – Plasmacytoid DCs	Rabbit (Santacruz) (1:50)	Donkey anti rabbit-488(Invitrogen) /1: 500	Sc-681 / V-18
Cd11c – Myeloid DCs	Rabbit (LS Bio) (1:25)	Donkey antirabbit-488 (Invitrogen) /1: 500	LS C165321 / Polyclonal
CD4 – T Cells	Rabbit (abcam) (1:100)	Donkey antirabbit-488 (Invitrogen) /1: 500	ab133616 / EPR6855

References:

1. Kasturi, S. P. *et al.* Adjuvanting a Simian Immunodeficiency Virus Vaccine with Toll-Like Receptor Ligands Encapsulated in Nanoparticles Induces Persistent Antibody Responses and Enhanced Protection in TRIM5α Restrictive Macaques. *J. Virol.* **91**, (2017).